RESEARCH ARTICLE

Rapid and Sensitive RT-QuIC Detection of Human Creutzfeldt-Jakob Disease Using Cerebrospinal Fluid

Christina D. Orrú,[a] Bradley R. Groveman,[a] Andrew G. Hughson,[a] Gianluigi Zanusso,[b] Michael B. Coulthart,[c] Byron Caughey[a]

Laboratory of Persistent Viral Diseases, Rocky Mountain Laboratories, National Institute for Allergy and Infectious Diseases, National Institutes of Health, Hamilton, Montana, USA[a]; Department of Neurological and Movement Sciences, University of Verona, Verona, Italy[b]; Canadian CJD Surveillance System, Public Health Agency of Canada, Ottawa, Ontario, Canada[c]

C.D.O., B.R.G., and A.G.H. contributed equally to this study.

ABSTRACT **Fast, definitive diagnosis of Creutzfeldt-Jakob disease (CJD) is important in assessing patient care options and transmission risks. Real-time quaking-induced conversion (RT-QuIC) assays of cerebrospinal fluid (CSF) and nasal-brushing specimens are valuable in distinguishing CJD from non-CJD conditions but have required 2.5 to 5 days. Here, an improved RT-QuIC assay is described which identified positive CSF samples within 4 to 14 h with better analytical sensitivity. Moreover, analysis of 11 CJD patients demonstrated that while 7 were RT-QuIC positive using the previous conditions, 10 were positive using the new assay. In these and further analyses, a total of 46 of 48 CSF samples from sporadic CJD patients were positive, while all 39 non-CJD patients were negative, giving 95.8% diagnostic sensitivity and 100% specificity. This second-generation RT-QuIC assay markedly improved the speed and sensitivity of detecting prion seeds in CSF specimens from CJD patients. This should enhance prospects for rapid and accurate *ante mortem* CJD diagnosis.**

IMPORTANCE **A long-standing problem in dealing with various neurodegenerative protein misfolding diseases is early and accurate diagnosis. This issue is particularly important with human prion diseases, such as CJD, because prions are deadly, transmissible, and unusually resistant to decontamination. The recently developed RT-QuIC test allows for highly sensitive and specific detection of CJD in human cerebrospinal fluid and is being broadly implemented as a key diagnostic tool. However, as currently applied, RT-QuIC takes 2.5 to 5 days and misses 11 to 23% of CJD cases. Now, we have markedly improved RT-QuIC analysis of human CSF such that CJD and non-CJD patients can be discriminated in a matter of hours rather than days with enhanced sensitivity. These improvements should allow for much faster, more accurate, and practical testing for CJD. In broader terms, our study provides a prototype for tests for misfolded protein aggregates that cause many important amyloid diseases, such as Alzheimer's, Parkinson's, and tauopathies.**

Received 5 December 2014 **Accepted** 9 December 2014 **Published** 20 January 2015

Citation Orrú CD, Groveman BR, Hughson AG, Zanusso G, Coulthart MB, Caughey B. 2015. Rapid and sensitive RT-QuIC detection of human Creutzfeldt-Jakob disease using cerebrospinal fluid. mBio 6(1):e02451-14. doi:10.1128/mBio.02451-14.

Editor Reed B. Wickner, National Institutes of Health

Address correspondence to Byron Caughey, bcaughey@nih.gov.

This article is a direct contribution from a Fellow of the American Academy of Microbiology.

Among the numerous mammalian prion diseases or transmissible spongiform encephalopathies (TSEs) is human Creutzfeldt-Jakob disease (CJD), an incurable, fatal neurodegenerative disease. CJD can have genetic and acquired origins, but the most common form is sporadic CJD (sCJD), which arises without an identifiable genetic or infectious cause in about one person per million per year worldwide. Although sCJD is not contagious, it is transmissible to experimental animals and can be transmitted to other humans by iatrogenic routes, such as corneal transplants, neurosurgical procedures using contaminated instruments, or growth hormone administration (for review, see reference 1).

The molecular pathogenesis of TSEs involves the accumulation of abnormal, infectivity-associated forms of prion protein (PrP) which serve as disease-specific markers. While the normal form of PrP, PrP^{Sen}, is mostly monomeric, protease sensitive, and rich in α-helices (2, 3), TSE-associated forms (e.g., PrP^{CJD}) tend to be multimeric (4–7), relatively protease resistant (8), and rich in β-sheet (2, 9–12). The extent of the protease-resistant core of PrP^{CJD} (e.g., type 1 or 2) and the patient's alleles at *PRNP* codon 129 (encoding methionine [M] or valine [V]) define six different sCJD subtypes, namely, MM1, MM2, MV1, MV2, VV1, and VV2 (for review, see reference 13).

The ability of TSE-associated forms of PrP, such as PrP^{CJD}, to seed the polymerization of recombinant PrP^{Sen} ($rPrP^{Sen}$) into amyloid fibrils that enhance the fluorescence of thioflavin T (ThT) serves as the basis of sensitive assays for prion-associated seeding activity (14–16). One of these assays, real-time quaking-induced conversion (RT-QuIC), is often at least as sensitive as animal bioassays and useful for detecting prion-seeding activity in a wide variety of tissues and fluids from TSE-infected hosts (15, 16). Quantitation of relative levels of prion-seeding activity can be achieved using endpoint dilution RT-QuIC (15) or, under more

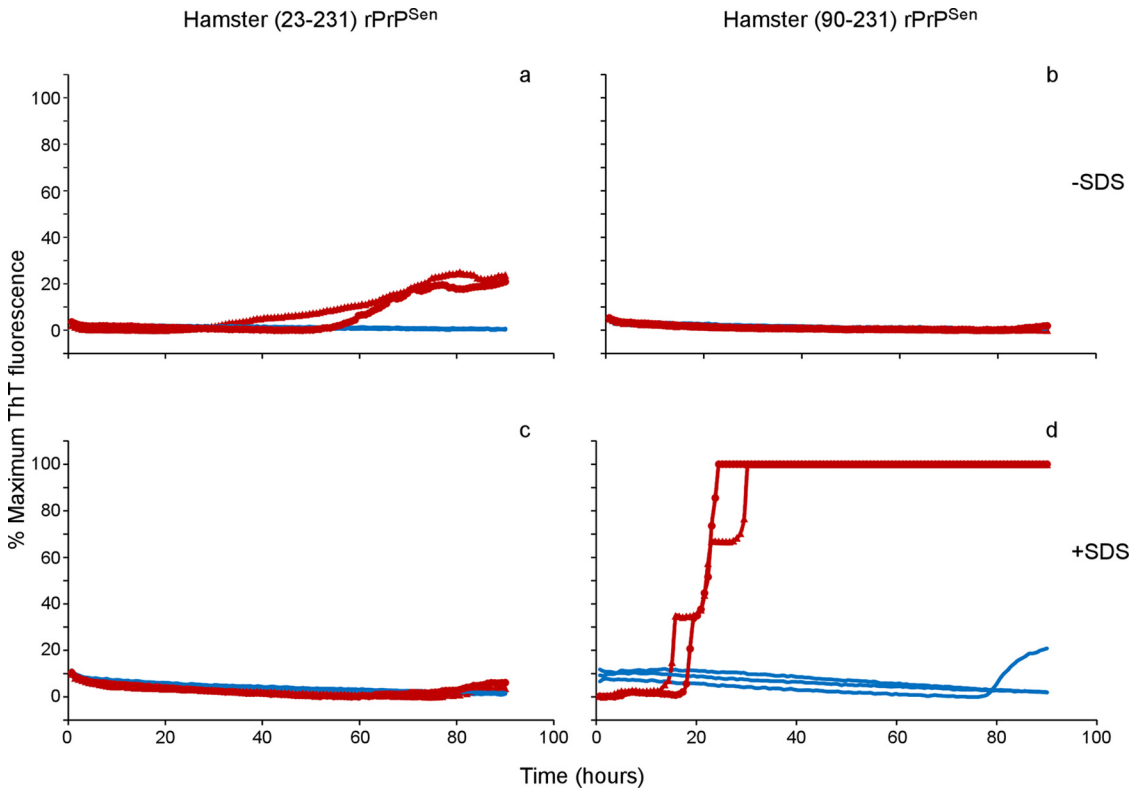

FIG 1 Comparison of CSF RT-QuIC analyses using rHaPrP^{Sen} 23–231 or 90–231, with or without SDS. Two sCJD samples (red) and three nonneurological control CSF samples (blue) were tested at 42°C by using full-length rHaPrP^{Sen} 23–231 (left) or truncated rHaPrP^{Sen} 90–231 (right) with (bottom) or without (top) the addition of 0.002% SDS. Distinct symbols represent separate sCJD samples. In the reaction mixtures containing rHaPrP^{Sen} 90–231 and SDS (bottom right), one of the three nonneurological control samples showed prion-independent fibril formation near 80 h, but this is more than 50 h after the established cutoff time point for these conditions (see Materials and Methods). Symbols show the mean fluorescence from four technical replicate wells.

carefully controlled experimental conditions, comparisons of reaction kinetics (17).

RT-QuIC testing of human cerebrospinal fluid (CSF) (18–20) and olfactory mucosa (21) can be highly sensitive and specific in discriminating sporadic and genetic CJD patients from non-CJD controls. Because the current alternatives for definitive diagnosis of CJD based on PrP^{CJD} detection in living patients require brain biopsies, RT-QuIC analysis of CSF is being broadly implemented as a key diagnostic tool. However, one of the practical limitations of current versions of the assay is that it typically takes 2.5 to 5 days to analyze most samples of diagnostic significance, such as human CSF (18, 19) and olfactory mucosa (21). Furthermore, extensive RT-QuIC analyses of CSF samples have shown that despite having 99 to 100% diagnostic specificity, the assay has failed to identify 11 to 23% of sporadic CJD cases (18, 19). Our recent exploratory study of olfactory brushings by RT-QuIC increased diagnostic sensitivity to ≥97% (21), but this sampling procedure awaits larger-scale validation and implementation. In contrast, CSF samples are routinely collected from patients with suspected CJD as part of screening for neurological disorders that mimic CJD but are potentially treatable (22). Thus, CSF remains a primary diagnostic sample for testing by RT-QuIC. In this light, improvement of the sensitivity of CSF testing by RT-QuIC is needed to provide more accurate diagnostic information to guide decisions about treating patients and reducing risks of iatrogenic CJD transmissions. In the present study, we have markedly improved RT-QuIC detection of prion-seeding activity in human CSF such that CJD and non-CJD patients can be discriminated in a matter of hours rather than days with enhanced sensitivity.

RESULTS

Enhanced detection of sCJD with CSF RT-QuIC by using truncated substrate and SDS. For RT-QuIC-based sCJD diagnosis using CSF samples, full-length human or hamster rPrP^{Sen} substrates (residues 23 to 231, i.e., Hu or Ha rPrP^{Sen} 23–231, respectively) have been used successfully (18, 19). Here, we tested whether an N-terminally truncated hamster rPrP^{Sen} (residues 90 to 231, i.e., Ha rPrP^{Sen} 90–231) might also improve sCJD detection in CSF samples. Instead, we found initially that when pure CSF was analyzed, positive reactions occurred only with the full-length substrate (compare Fig. 1A and B). However, pure CSF specimens lack SDS that was present in the previously studied brain homogenates, so we also tested the effects of SDS on CSF-seeded reaction mixtures using each of the substrates. Although with Ha rPrP^{Sen} 23–231, 0.002% SDS decreased the RT-QuIC responses to CSF samples from two patients with definite sCJD (Fig. 1C), it markedly enhanced the speed and strength of reactions containing Ha rPrP^{Sen} 90–231 (Fig. 1D). Thus, combining Ha rPrP^{Sen} 90–231 with SDS gave more rapid and robust RT-QuIC responses to sCJD seeds in CSF than has been observed with previously described conditions (18, 19).

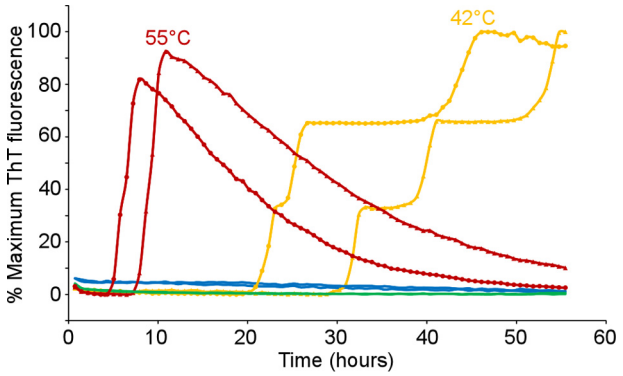

FIG 2 Increased temperature accelerated RT-QuIC detection of sCJD in CSF. Comparison of individual CSF samples (circles or triangles) at either 42°C (gold) or 55°C (red) using the rHaPrP^{Sen} 90–231 substrate in the presence of 0.002% SDS. Negative controls are displayed for both 42°C (blue lines) and 55°C (green line). The symbols represent the means from four technical replicate reactions.

Further acceleration of sCJD CSF RT-QuIC with increased temperature. To further improve upon the new conditions described above (containing SDS and rHaPrP^{Sen} 90–231), we increased the RT-QuIC reaction temperature from 42°C to 55°C. The higher incubation temperature reduced the lag phase of reactions seeded with sCJD CSF by at least 4-fold, without eliciting false-positive responses in the reactions seeded with non-CJD CSF (Fig. 2).

New conditions for CSF RT-QuIC improve speed and sensitivity of sCJD detection. We then applied RT-QuIC using the combination of the rHaPrP^{Sen} 90–231 substrate, 55°C, and 0.002% SDS (referred to here as improved QuIC-CSF [IQ-CSF] conditions) to an initial panel of 11 CSF samples from probable and definite sCJD patients. This panel included the following sCJD subtypes: MM1 ($n = 3$), MV1 ($n = 1$), VV2 ($n = 1$), MM ($n = 2$), MV ($n = 1$), and VV ($n = 1$) of unknown PrP^{CJD} type and two of unknown *PRNP* genotype (Fig. 3). We also tested the same samples in parallel using the RT-QuIC conditions that were established previously for sCJD diagnosis using CSF samples, i.e., Ha rPrP^{Sen} 23–231, 42°C, and no SDS (referred to here as previous QuIC-CSF [PQ-CSF] conditions) (19). Ten of 11 sCJD samples tested with the IQ-CSF conditions gave strong positive reactions in less than 10 h (Fig. 3, red circles). In contrast, with the PQ-CSF conditions, only 7 of 11 of the samples gave positive reactions within 90 h, with much slower reaction kinetics and weaker overall fluorescence enhancements (Fig. 3, blue triangles). Notably, of the 4 samples that did not give positive responses under the PQ-CSF conditions, 3 gave strong and rapid responses using the IQ-CSF conditions (Fig. 3C, D, F, and G), while samples from non-CJD control cases remained negative (Fig. 3L). These findings provided initial evidence that our new reaction conditions improve the speed and diagnostic sensitivity of RT-QuIC using CSF samples.

CSF endpoint dilution analysis using new RT-QuIC conditions. To directly compare the analytical sensitivities of RT-QuIC using the PQ-CSF and IQ-CSF conditions, we tested serial dilutions of 4 sCJD CSF samples that gave positive reactions under both conditions in the above-described analyses (Fig. 4). Four replicate reactions were tested per sample. Using Spearman-Karber analysis of the data (23), we estimated the volume of pure CSF required to give 50% positive replicate wells under each condition (the 50% seeding dose [SD_{50}]). For 3 of the patients' specimens, the required volume was 5- to 36-fold lower using the new IQ-CSF conditions while being nearly equivalent for the 4th specimen. Thus, these endpoint dilution measurements confirmed that, in the majority of cases, the IQ-CSF conditions provided not only faster but also more analytically sensitive RT-QuIC reactions than did PQ-CSF conditions.

Analysis of an additional blinded panel of CJD and non-CJD CSF samples. For further evaluation of the performance of the IQ-CSF conditions, we tested another 76 CSF samples from probable or definite sCJD patients as well as both neurological disease and healthy controls to give a total sample size of 87. Table 1 summarizes characteristics of all of the cases and controls tested with the IQ-CSF conditions so far. Figure 5 shows the RT-QuIC results from the sCJD (red) and non-CJD (orange) samples. Consistent with the results in Fig. 3, we saw rapid and strong responses from 46 of 48 sCJD CSF samples using the IQ-CSF conditions (Fig. 5A and B), while 1 definite sCJD (MM1) CSF sample, 1 probable sCJD (type unknown) CSF sample, and all 39 negative non-CJD controls gave no ThT fluorescence enhancement within 55 h, according to positivity criteria described in Materials and Methods. The peak relative fluorescence values from the individual sCJD and non-CJD samples are shown in Fig. 5B, and the lag times to the threshold for positive responses are shown in Fig. 5C. For many of these samples, we lacked enough volume to also test them with the PQ-CSF conditions, but these conditions have already been tested extensively (19, 21). Thus, for comparison of the PQ-CSF conditions to our present IQ-CSF assay results, we show data derived from our previously published analyses of an overlapping panel of CSF samples (21), which indicated much slower and weaker RT-QuIC responses than those obtained with the new conditions (Fig. 5A and C). Furthermore, with the latter conditions, 85% of the sCJD CSF samples gave positive reactions in all of their individual replicate reactions, whereas this was true of only 38% of the sCJD samples tested using the PQ-CSF conditions (data not shown). Overall, the positive RT-QuIC tests from 46/48 sCJD cases using the IQ-CSF conditions indicated a sensitivity of 96% (95% confidence interval [CI] = 85 to 99%). By comparison, the sensitivity that we have obtained using the PQ-CSF conditions was 77% (CI = 57 to 89%) (21), which was significantly lower ($P = 0.02$ by two-sided Fisher exact test) than our sensitivity with the IQ-CSF conditions. The negative responses from all of the non-CJD samples indicated a nominal specificity of 100% (CI = 89 to 100%), which is consistent with data from previously described RT-QuIC conditions (18, 19, 21). Taken together, these results indicated that the new IQ-CSF conditions improved the speed and sensitivity of the RT-QuIC CSF assay for sCJD while maintaining full specificity.

DISCUSSION

Improved *ante mortem* diagnostic testing for CJD would have significant value in medical and public health practice for several reasons. Although quick and accurate diagnoses are helpful in dealing with any disease, rapid detection of CJD infections is particularly important in order to prevent iatrogenic transmissions. A recurring scenario is one that occurred recently in two different United States hospitals: medical instruments were used on CJD-infected patients and then on many other individuals before CJD was suspected in the original patients. Because routine disinfec-

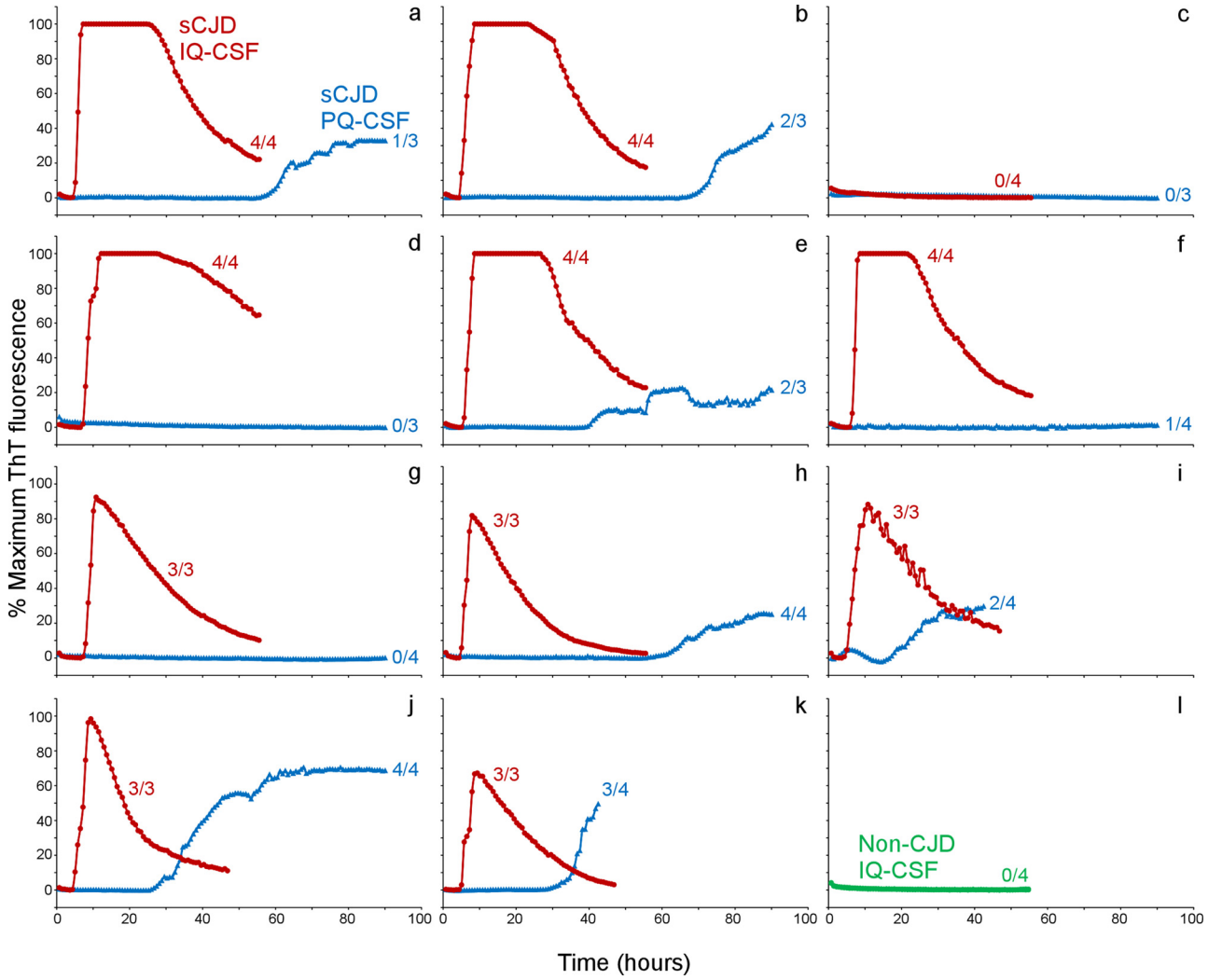

FIG 3 Comparison of PQ-CSF and IQ-CSF RT-QuIC analyses of individual sCJD and negative-control CSF samples. CSFs were tested with either the IQ-CSF (red circles) or PQ-CSF (blue triangles) conditions. The latter data have been reported previously (21). Traces from 2 non-neurological control (NNC) samples analyzed with the IQ-CSF conditions are reported in panel l (green circles). Due to technical issues, traces in panels i and k end at 45 h. Nevertheless, using both conditions, these samples were called positive based on the criteria established in Materials and Methods. Symbols indicate the means from three or four replicate wells. Color-matched fractions indicate the number of positive wells out of the total number of replicate reactions for each sample.

tion procedures are not adequate for CJD decontamination, such incidents can create risks of secondary hospital exposures (24). CJD remains untreatable, but accurate testing that can either rule in or rule out the disease should help to guide decisions about treatment options. With a progressive disease like CJD, the earlier the diagnosis can be established, the more likely it is that effective treatments can be developed. Finally, epidemiological surveillance of CJD, which currently relies heavily on autopsy-based diagnosis, could be more efficient, cost-effective, and broadly applicable with RT-QuIC testing of samples that can be obtained without autopsies.

Multiple CJD diagnostic laboratories around the world are implementing and validating RT-QuIC testing for human sCJD CSF using conditions similar to our PQ-CSF conditions (e.g., see references 19 and 21). Other major centers have also extensively evaluated other RT-QuIC conditions for CJD testing, including full-length human rPrP^{Sen} (residues 23 to 231) as the substrate, 37°C, and no SDS (18, 20) or a chimeric hamster-sheep rPrP^{Sen} (residues 14 to 231), 42°C, and no SDS (25). For each of these previously described conditions, the vast majority of the RT-QuIC-positive reaction mixtures seeded with human sCJD CSF samples become positive between 24 and 90 h. Our new conditions reduce that time to 4 to 14 h while increasing sensitivity relative to our own testing using the PQ-CSF conditions. Other previous studies using PQ-CSF-like conditions but with different instruments, shaking motions, and speeds have obtained somewhat higher diagnostic sensitivities (89% [CI = 83 to 95%]) (19). Determining whether the latter sensitivity is significantly lower than our current 96% (CI = 85 to 99%) sensitivity with the IQ-CSF conditions will require comparisons of much larger sample sets. However, it is clear that compared on identical instruments, the IQ-CSF conditions markedly improved not only the speed but also the analytical and diagnostic sensitivities of RT-QuIC analysis of CSF samples.

The mechanistic reasons for the improvements with the IQ-

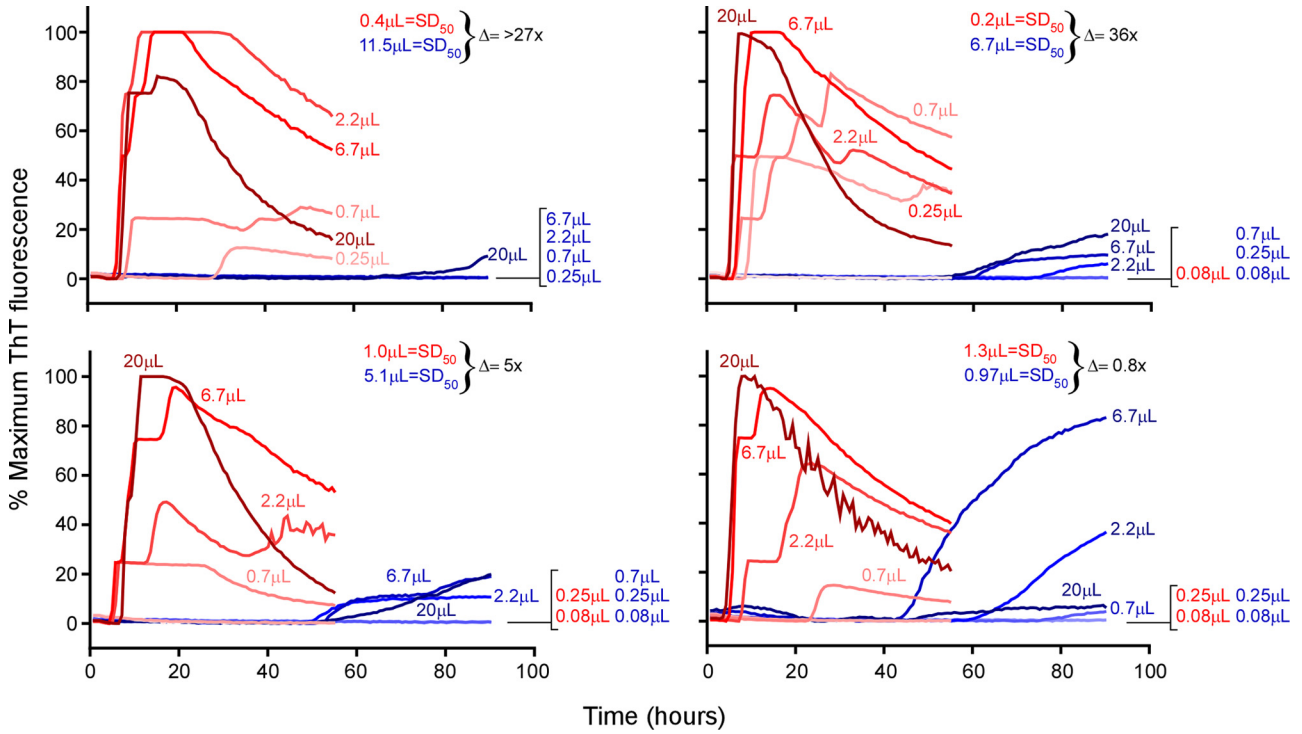

FIG 4 Endpoint dilution analyses of 4 sCJD CSF samples using PQ-CSF and IQ-CSF conditions. Reaction mixtures seeded with serial dilutions of sCJD CSF samples (20- to 0.08-μl equivalents of pure CSF as designated) were tested with the PQ-CSF (shades of blue) and IQ-CSF (shades of red) conditions. Each panel shows results from an individual sCJD patient specimen. Spearman-Karber estimates of the volume of pure CSF equivalents giving 50% positive replicate wells (SD_{50}) under the IQ-CSF (red) or PQ-CSF (blue) conditions are also indicated. The fold difference in the SD_{50} values (black, Δ) indicates the relative analytical sensitivities obtained under the PQ-CSF and IQ-CSF conditions for the given sCJD CSF specimen. Individual traces represent means from four replicate reactions.

CSF conditions are not clear and are likely to be complex. With respect to the hamster $rPrP^{Sen}$ substrate, our data indicated that removal of unstructured N-terminal residues 23 to 89 allowed for much faster sCJD CSF-seeded reactions, but only when the reaction mixture is supplemented with SDS (Fig. 1). Paradoxically, the addition of SDS to reaction mixtures with the full-length hamster $rPrP^{Sen}$ substrate inhibited the reactions. Thus, there appears to be a synergistic beneficial effect of adding SDS and removing $rPrP^{Sen}$ 23–89. Because the effect of SDS is dependent on the type of $rPrP^{Sen}$, it is likely that the detergent is affecting the substrate rather than the sCJD seeds in CSF. We note that increasing SDS above 0.002% was detrimental to the speed and intensity of sCJD CSF-seeded RT-QuIC responses (data not shown). Beyond that, we can only speculate that the combined effects of SDS and sub-

TABLE 1 CSF RT-QuIC, 14-3-3, and Tau results with clinical and demographic profiles of sCJD and negative-control patients

Patient type	No. of positive samples/total no. of samples			Age in yrs ± SD	Gender
	IQ-CSF RT-QuIC assay	14-3-3 assay	Tau assay (>2,400 pg/ml)		
sCJD patients[a]	46/48	47/48	40/47	68 ± 11	Male, 22; female, 26
MM1	17/18	18/18	16/17		
MV1	7/7	7/7	5/7		
MV2	5/5	4/5	1/5		
VV2	7/7	7/7	7/7		
ND1	6/6	6/6	6/6		
MM	2/2	2/2	2/2		
MV	1/1	1/1	1/1		
VV	1/1	1/1	1/1		
ND	0/1	1/1	1/1		
Control patients[b]	0/39	3/34	0/36	69 ± 11	Male, 17; female, 22
Neurological	0/30	3/28	0/30		
Nonneurological	0/9	0/6	0/6		

[a] When available, the patients' protein gene (*PRNP*) codon 129, heterozygous or homozygous for methionine (M) or valine (V), and the classification of the protease-resistant core of PrPCJD (type 1 or 2) are reported. Patients who were not genotyped were classified as not done (ND).

[b] Control patients were classified as either "non-neurological," displaying no neurological symptoms at the time of CSF collection, or "neurological." Neurological patients had a mixture of diagnoses, as listed in Materials and Methods.

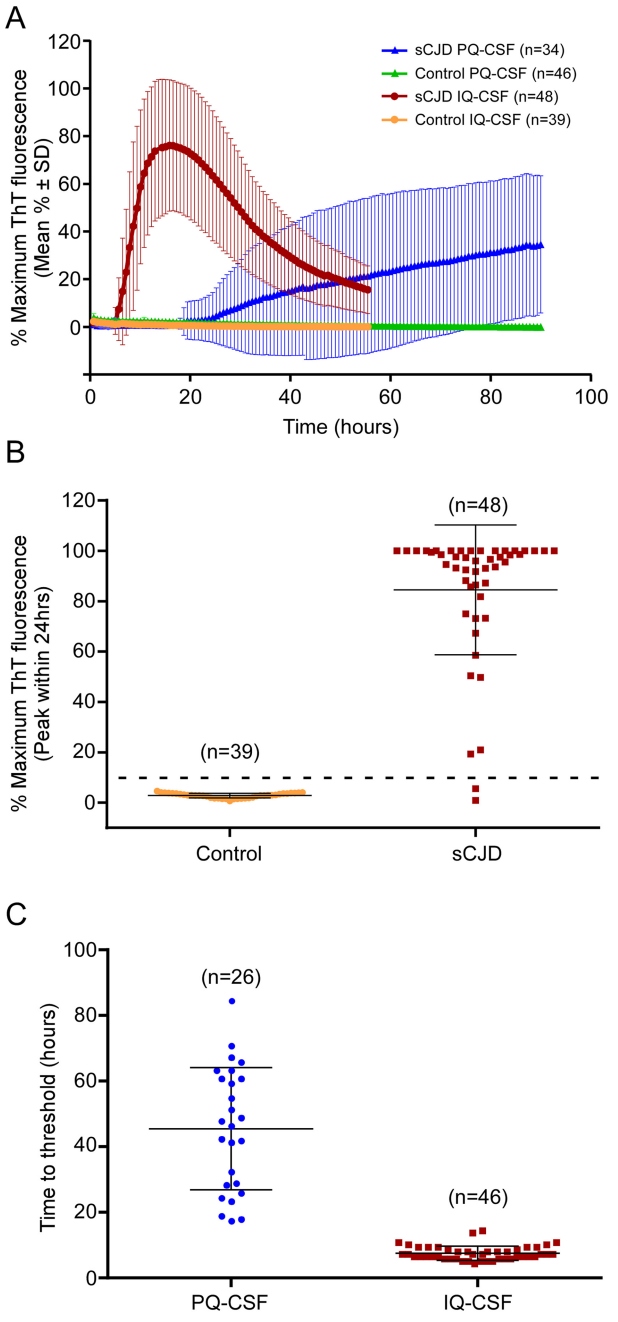

FIG 5 Averaged kinetics, peak fluorescence, and times to threshold using PQ-CSF and/or IQ-CSF conditions. (A) Averaged RT-QuIC kinetics for sCJD and non-CJD CSF samples. Mean ThT fluorescence for all tested CSF specimens from non-CJD control (green and orange) and sCJD (blue and red) patients under PQ-CSF (triangles) or IQ-CSF (circles) conditions are shown. Traces denote the means (±standard deviation [SD]) from biological replicates for each category as indicated by the legend. Each biological replicate was in turn an average from three or four technical replicate wells. PQ-CSF data were previously reported (21). (B) Peak fluorescence values for CSF samples analyzed with the IQ-CSF protocol. The average peak fluorescence value from all 48 sCJD samples (red squares) and 39 control samples (orange circles) tested blinded using the IQ-CSF conditions is shown for each individual sample with mean (horizontal line) and standard deviations (vertical lines). The dashed line indicates the positivity threshold (see Materials and Methods). (C) Times to threshold (defined in Materials and Methods) for individual sCJD RT-QuIC-positive CSF samples tested with the PQ-CSF (blue circles; derived from previously reported experiments [21]) or IQ-CSF (red squares) conditions (this study) are shown. The mean (horizontal line) and standard deviations (vertical lines) are displayed for each testing condition.

strate truncation might alter one or more of the following: substrate stability, the formation of on- or off-pathway states or intermediates, the interactions between seed and substrate, and/or the stability or seeding capacity of the nascent rPrP amyloid product. With respect to temperature, we expect that higher temperatures could destabilize the substrate to make it more rapidly convertible to amyloid, increase the intermolecular collisions between seed and substrate, or promote secondary nucleation by promoting shearing of nascent rPrP amyloid fibrils to generate more seeding sites. Much additional study will be required to distinguish among these many possibilities.

MATERIALS AND METHODS

Cerebrospinal fluid samples. Cerebrospinal fluid samples (>0.5 ml) were obtained from patients with possible or probable Creutzfeldt-Jakob disease at the time of sampling, as well as from the patients with other neurologic disorders, including Alzheimer's disease (6 patients), amyotrophic lateral sclerosis (4 patients), atypical Parkinsonism (1 patient), dementia (2 patients), dystonia (1 patient), encephalitis (1 patient), frontotemporal dementia (3 patients), Lewy body dementia (1 patient), mild cognitive impairment (7 patients), myclonus (1 patient), or rapidly progressive dementia (3 patients) (Table 1). Nonneurological cerebrospinal fluid control samples were purchased from Innovative Research or obtained from the Neuropathology Laboratory at Verona University Hospital. All cerebrospinal fluid samples were stored at −80°C from a time shortly after harvest until use in this assay.

The study was approved by the ethics committee at Istituto Superiore di Sanità (Italy), which is recognized by the Office for Human Research Protections of the U.S. Department of Health and Human Services. Informed consent for participation in research was obtained in accordance with the Declaration of Helsinki and the Additional Protocol to the Convention on Human Rights and Biomedicine, concerning Biomedical Research. All the sampling of CSF was performed after informed consent was obtained from each patient or the patient's representative. The analyses of human specimens that were performed at the NIAID were performed under exemption number 11517 for the use of encoded samples from the NIH Office of Human Subjects Research Protections.

Recombinant prion protein purification. Recombinant PrP was prepared as previously described (15). Briefly, *Escherichia coli* carrying the vector with the PrP sequence (Syrian hamster residues 23 to 231 [GenBank accession number K02234] or residues 90 to 231) was grown in Luria broth (LB) medium in the presence of kanamycin and chloramphenicol. Protein expression was induced using Overnight Express autoinduction system 1 (Novagen). Recombinant PrP was purified from inclusion bodies under denaturing conditions using Ni-nitrilotriacetic acid (NTA) superflow resin (Qiagen) with an ÄKTA fast protein liquid chromatographer (FPLC). The protein was refolded on the column using a guanidine HCl reduction gradient and eluted using an imidazole gradient as described (15). The purified protein was extensively dialyzed into 10 mM sodium phosphate buffer (pH 5.8). Protein concentration was determined by absorbance measured at 280 nm. Following filtration (0.22-μm syringe filter [Fisher]), recombinant PrP was aliquoted and stored at −80°C. Prior to use, the protein was filtered again (100-kDa spin filter [Pall]), and the concentration was again determined.

RT-QuIC. Real-time QuIC (RT-QuIC) assays were performed as reported previously for CSF (21) except where indicated. Briefly, the basic RT-QuIC reaction mix contained 10 mM phosphate buffer (pH 7.4), 300 mM NaCl, 0.1 mg/ml $rPrP^{Sen}$, 10 μM thioflavin T (ThT), and 1 mM ethylenediaminetetraacetic acid tetrasodium salt (EDTA). Reactions were run with either Ha $rPrP^{Sen}$ 23–231 or 90–231 with or without the addition of 0.002% SDS to the reaction mix. Eighty microliters of reaction mix was loaded into a black 96-well plate with a clear bottom (Nunc), and reaction mixtures were seeded with 20 μl of CSF for a final reaction volume of 100 μl. Plates were sealed (Nalgene Nunc International sealer) and incubated in a BMG FLUOstar Omega plate reader at either 42 or 55°C for 55

to 90 h with cycles of 60 s of shaking (700 rpm, double-orbital) and 60 s of rest throughout the incubation. ThT fluorescence measurements (excitation, 450 ± 10 nm; emission, 480 ± 10 nm [bottom read]) were taken every 45 min.

Data analysis. To compensate for minor differences between fluorescence plate readers, including baseline differences, we normalized the values to a percentage of the maximal fluorescence response of the plate readers as described (21). These normalized values were plotted versus reaction time.

Samples were judged to be RT-QuIC positive by using criteria similar to those previously described for RT-QuIC analyses of CSF specimens (19, 21), using baseline-adjusted, normalized fluorescence values and suitably adjusted cutoff values (21). Our discrimination criteria are briefly described as follows. The threshold was calculated as the mean value at the time of assessment from all negative-control samples plus 10 standard deviations. However, given the signal strength and rapid response, a stricter threshold of 10% was set beyond the calculated threshold to decrease the likelihood of false positives. A sample was considered positive if the mean of the highest two normalized fluorescence values from replicate wells was higher than a predetermined threshold and at least two out of four replicate wells crossed that threshold (21). If only three replicate wells were run, then only the average value of all three wells was considered. For PQ-CSF conditions, positive/negative assessments were made at the 90-h time point. For IQ-CSF conditions, positive/negative results were scored based on the highest peak value prior to 24 h to account for the signal degradation over time. For sensitivity determinations, IQ-CSF conditions were assessed out to 55 h.

ACKNOWLEDGMENTS

This work was supported by the Intramural Research Program of the NIAID and in part by the Alliance Biosecure Foundation.

We thank Suzette Priola, Gerald Baron, and Clayton Winkler for critical evaluation of the manuscript and Anita Mora for graphics assistance.

REFERENCES

1. **Brown P, Brandel JP, Sato T, Nakamura Y, Mackenzie J, Will RG, Ladogana A, Pocchiari M, Leschek EW, Schonberger LB.** 2012. Iatrogenic Creutzfeldt-Jakob disease, final assessment. Emerg Infect Dis **18:** 901–907. http://dx.doi.org/10.3201/eid1806.120116.
2. **Pan K-M, Baldwin M, Nguyen J, Gasset M, Serban A, Groth D, Mehlhorn I, Huang Z, Fletterick RJ, Cohen FE, Prusiner SB.** 1993. Conversion of alpha-helices into beta-sheets features in the formation of the scrapie prion protein. Proc Natl Acad Sci U S A **90:**10962–10966. http://dx.doi.org/10.1073/pnas.90.23.10962.
3. **Riek R, Hornemann S, Wider G, Billeter M, Glockshuber R, Wüthrich K.** 1996. NMR structure of the mouse prion protein domain PrP(121–231). Nature **382:**180–182. http://dx.doi.org/10.1038/382180a0.
4. **Diringer H, Gelderblom H, Hilmert H, Ozel M, Edelbluth C, Kimberlin RH.** 1983. Scrapie infectivity, fibrils and low molecular weight protein. Nature **306:**476–478. http://dx.doi.org/10.1038/306476a0.
5. **Prusiner SB, McKinley MP, Bowman KA, Bendheim PE, Bolton DC, Groth DF, Glenner GG.** 1983. Scrapie prions aggregate to form amyloid-like birefringent rods. Cell **35:**349–358. http://dx.doi.org/10.1016/0092-8674(83)90168-X.
6. **Caughey B, Kocisko DA, Raymond GJ, Lansbury PT.** 1995. Aggregates of scrapie associated prion protein induce the cell-free conversion of protease-sensitive prion protein to the protease-resistant state. Chem Biol **2:**807–817. http://dx.doi.org/10.1016/1074-5521(95)90087-X.
7. **Silveira JR, Raymond GJ, Hughson AG, Race RE, Sim VL, Hayes SF, Caughey B.** 2005. The most infectious prion protein particles. Nature **437:**257–261. http://dx.doi.org/10.1038/nature03989.
8. **McKinley MP, Bolton DC, Prusiner SB.** 1983. A protease-resistant protein is a structural component of the scrapie prion. Cell **35:**57–62. http://dx.doi.org/10.1016/0092-8674(83)90207-6.
9. **Caughey BW, Dong A, Bhat KS, Ernst D, Hayes SF, Caughey WS.** 1991. Secondary structure analysis of the scrapie-associated protein PrP 27–30 in water by infrared spectroscopy. Biochemistry **30:**7672–7680. http://dx.doi.org/10.1021/bi00245a003.
10. **Safar J, Roller PP, Gajdusek DC, Gibbs CJ, Jr.** 1993. Conformational transitions, dissociation, and unfolding of scrapie amyloid (prion) protein. J Biol Chem **268:**20276–20284.
11. **Smirnovas V, Baron GS, Offerdahl DK, Raymond GJ, Caughey B, Surewicz WK.** 2011. Structural organization of brain-derived mammalian prions examined by hydrogen-deuterium exchange. Nat Struct Mol Biol **18:**504–506. http://dx.doi.org/10.1038/nsmb.2035.
12. **Baron GS, Hughson AG, Raymond GJ, Offerdahl DK, Barton KA, Raymond LD, Dorward DW, Caughey B.** 2011. Effect of glycans and the glycophosphatidylinositol anchor on strain dependent conformations of scrapie prion protein: improved purifications and infrared spectra. Biochemistry **50:**4479–4490. http://dx.doi.org/10.1021/bi2003907.
13. **Parchi P, de Boni L, Saverioni D, Cohen ML, Ferrer I, Gambetti P, Gelpi E, Giaccone G, Hauw JJ, Höftberger R, Ironside JW, Jansen C, Kovacs GG, Rozemuller A, Seilhean D, Tagliavini F, Giese A, Kretzschmar HA.** 2012. Consensus classification of human prion disease histotypes allows reliable identification of molecular subtypes: an inter-rater study among surveillance centres in Europe and USA. Acta Neuropathol **124:**517–529. http://dx.doi.org/10.1007/s00401-012-1002-8.
14. **Colby DW, Zhang Q, Wang S, Groth D, Legname G, Riesner D, Prusiner SB.** 2007. Prion detection by an amyloid seeding assay. Proc Natl Acad Sci U S A **104:**20914–20919. http://dx.doi.org/10.1073/pnas.0710152105.
15. **Wilham JM, Orrú CD, Bessen RA, Atarashi R, Sano K, Race B, Meade-White KD, Taubner LM, Timmes A, Caughey B.** 2010. Rapid end-point quantitation of prion seeding activity with sensitivity comparable to bioassays. PLoS Pathog **6:**e1001217. http://dx.doi.org/10.1371/journal.ppat.1001217.
16. **Atarashi R, Sano K, Satoh K, Nishida N.** 2011. Real-time quaking-induced conversion: a highly sensitive assay for prion detection. Prion **5:**150–153. http://dx.doi.org/10.4161/pri.5.3.16893.
17. **Shi S, Mitteregger-Kretzschmar G, Giese A, Kretzschmar HA.** 2013. Establishing quantitative real-time quaking-induced conversion (qRT-QuIC) for highly sensitive detection and quantification of PrPSc in prion-infected tissues. Acta Neuropathol Commun **1:**44. http://dx.doi.org/10.1186/2051-5960-1-44.
18. **Atarashi R, Satoh K, Sano K, Fuse T, Yamaguchi N, Ishibashi D, Matsubara T, Nakagaki T, Yamanaka H, Shirabe S, Yamada M, Mizusawa H, Kitamoto T, Klug G, McGlade A, Collins SJ, Nishida N.** 2011. Ultrasensitive human prion detection in cerebrospinal fluid by real-time quaking-induced conversion. Nat Med **17:**175–178. http://dx.doi.org/10.1038/nm.2294.
19. **McGuire LI, Peden AH, Orrú CD, Wilham JM, Appleford NE, Mallinson G, Andrews M, Head MW, Caughey B, Will RG, Knight RS, Green AJ.** 2012. RT-QuIC analysis of cerebrospinal fluid in sporadic Creutzfeldt-Jakob disease. Ann Neurol **72:**278–285. http://dx.doi.org/10.1002/ana.23589.
20. **Sano K, Satoh K, Atarashi R, Takashima H, Iwasaki Y, Yoshida M, Sanjo N, Murai H, Mizusawa H, Schmitz M, Zerr I, Kim YS, Nishida N.** 2013. Early detection of abnormal prion protein in genetic human prion diseases now possible using real-time QUIC assay. PLoS One **8:**e54915. http://dx.doi.org/10.1371/journal.pone.0054915.
21. **Orrú CD, Bongianni M, Tonoli G, Ferrari S, Hughson AG, Groveman BR, Fiorini M, Pocchiari M, Monaco S, Caughey B, Zanusso G.** 2014. A test for Creutzfeldt-Jakob disease using nasal brushings. N Engl J Med **371:**519–529. http://dx.doi.org/10.1056/NEJMoa1315200.
22. **Chitravas N, Jung RS, Kofskey DM, Blevins JE, Gambetti P, Leigh RJ, Cohen ML.** 2011. Treatable neurological disorders misdiagnosed as Creutzfeldt-Jakob disease. Ann Neurol **70:**437–444. http://dx.doi.org/10.1002/ana.22454.
23. **Dougherty RM.** 1964. Animal virus titration techniques, p 183437–186. In Harris RJC (ed), Techniques in experimental virology. Academic Press, New York, NY.
24. **Belay ED, Blase J, Sehulster LM, Maddox RA, Schonberger LB.** 2013. Management of neurosurgical instruments and patients exposed to Creutzfeldt-Jakob disease. Infect Control Hosp Epidemiol **34:**1272–1280. http://dx.doi.org/10.1086/673986.
25. **Cramm M, Schmitz M, Karch A, Zafar S, Varges D, Mitrova E, Schroeder B, Raeber A, Kuhn F, Zerr I. 9 May** 2014. Characteristic CSF prion seeding efficiency in humans with prion diseases. Mol Neurobiol. http://dx.doi.org/10.1007/s12035-014-8709-6.